The Conductive Behavior and Structural Characteristics in the I^+-Beam-Implanted Layer of Plasma-Polymerized Pyrrole Film

ZHI SHEN TONG,[1] MEI ZHEN WU,[1] TIAN SHU PU,[1] ZHENG YANG ZHANG,[1] JING ZHANG,[1] RUO PENG JIN,[1] DE ZHANG ZHU,[2] FU YING ZHU,[2] DE XIN CAO,[2] JIAN QING CAO[2]

[1] Department of Basic Sciences, China Textile University, Shanghai, 200051, China

[2] Shanghai Institute of Nuclear Research, Chinese Academy of Sciences, Shanghai, 201800, China

Received 11 July 1997; accepted 7 December 1997

ABSTRACT: A dense organic film was prepared by plasma polymerization of pyrrole. A 20 keV I^+ implantation at a fluence of 1×10^{16} ions cm^{-2} was used to produce a conducting surface layer due to doping. The characteristics of the implanted layer have been investigated using ion beam analysis techniques, X-ray photoelectron spectroscopy, and near-infrared to ultraviolet spectroscopy. The charge carriers transport in this implanted layer was also analyzed in the temperature region of 120 to 297 K. © 1998 John Wiley & Sons, Inc. J Appl Polym Sci 69: 1743–1751, 1998

Key words: pyrrole; plasma polymer; ion beam implantation; ion beam analysis; optical properties; electrical conductivity

INTRODUCTION

It is well known that the electrical conductivity of some polymers, with either conjugated or nonconjugated double bonds, can be drastically enhanced by doping.[1,2] Iodine as an acceptor is the effective dopant. The conductive behavior and the structural characteristics of the doped polymer are certainly of considerable interest, and have attracted much attention over the last decade. Despite the large amounts of work carried out, the details on these aspects are not yet well understood. It is apparent that these features depend on the conditions of both synthesis and doping. Recently, we prepared an organic film by plasma polymerization from pyrrole and investigated its composition and structural characteristics in detail.[3] Its conductivity can be enhanced by 11 orders of magnitude due to I^+-beam implantation. Our experimental result showed that this iodine-induced conduction is steady. In the present article, we determined the composition of the I^+-beam-implanted layer by ion-beam analysis techniques, Rutherford backscattering spectroscopy (RBS), and elastic recoil determination method (ERD), and ascertained the nature of iodine moiety with X-ray photoelectron spectroscopy (XPS). Furthermore, we calculated the complex refractive index, $N_l = n_l + ik_l$, for the I^+-beam-implanted layer by analyses of reflectance and transmittance data using the transfer matrix method. We then investigated further the optical properties of the implanted layer. It should be mentioned that because the thickness of the implanted layer was smaller than that of the pristine film, the calculation of optical constants for this layer was referred to a system consisting of two thin films and one thick plate: implanted layer *l*/pristine film layer *f*/substrate *s*. Finally, we explored the trans-

Correspondence to: Z. S. Tong.

Contract grant sponsor: National Natural Science Foundation of China; contract grant number: 19375036.

Journal of Applied Polymer Science, Vol. 69, 1743–1751 (1998)

© 1998 John Wiley & Sons, Inc. CCC 0021-8995/98/091743-09

port mechanism of charge carriers in the I^+-beam-implanted layer over the temperature region from 120 to 297 K.

EXPERIMENTAL

Plasma Polymerization

Plasma polymerization was performed in a glass-tube chamber with capacitive coupling at a frequency of 13.56 MHz. The schematic representation of the apparatus used for r.f. plasma polymerization is reported elsewhere.[3] The reaction chamber was evacuated to a pressure of 0.6 Pa before monomer ($C_4H_5N_1$) was introduced. Plasma polymer was deposited without using carrier gas; during the polymerization process, the total gaseous pressure was adjusted to 18 Pa via the regulation of the needle valve. The r.f. power and the rate of film growth were about 25 W and 0.5 nm s^{-1}, respectively. The density of deposited film was 1.9 kg m^{-3}, which is lower than that of plasma-polymerized thiophene film (3 kg m^{-3}) but similar to that of α-C film.[4,5]

I^+-Beam Implantation and Measurement

The plasma polymer film was implanted by an iodine-ion beam with the energy of 20 keV at a fluence 1×10^{16} ions cm^{-2}. The ion-beam current density was maintained below 0.2 μA cm^{-2} to avoid macroscopic heating of the sample. The composition of the sample deposited on silicon was determined by ion-beam analysis techniques (RBS and ERD). The incident energies of He^+ ions were 3 and 2 MeV for ERD and RBS, respectively.

The XPS measurement was performed on the sample deposited on aluminium with a MICRLAB MK II spectrometer utilizing Mg Kα radiation. The peak position (binding energy) was calibrated using the Ni $2p_{3/2}$ peak (852.65 eV) as a standard. The component analysis of the core-level spectrum was carried out on the spectrometer using a fitting program that permits the adjustment of parameters such as Gaussian-to-Lorentzian ratio, peak width, and peak position. The near-infrared (IR) to ultraviolet (UV) spectra for the sample on a quartz substrate were measured by a Perkin-Elmer Lambda 9UV-Vis-NIR spectrophotometer.

The conventional two-electrode technique was used to measure the direct current (dc) electrical resistance. The linear relation between the current and voltage indicated that the ohmic contacts were satisfying. The sheet resistances determined in the implanted layer were converted into bulk conductivities by using a conducting layer thickness evaluated from the full width at half maximum of the backscattering peak induced by iodine scattering in the RBS spectrum.

CALCULATION OF OPTICAL CONSTANTS

The complex-amplitude reflection and transmission coefficients of a pile of films have been reported by Harbecke as a product of transfer matrices.[6] We applied this method to the following situation: A plane electromagnetic wave is perpendicularly incident on a system of medium *a*/implanted layer *l*/pristine film layer *f*/substrate *s*/medium *b* (both media *a* and *b* are assumed to be vacuums). The substrate is sufficiently thick that light interferes incoherently between its front and back surfaces. Thus the reflectance (R) and transmittance (T) of this system are given by

$$R_{ab} = |r_{as}|^2 + \frac{|t_{as}t_{sa}\rho_{sb}\phi_s^2|^2}{1 - |r_{sa}\rho_{sb}\phi_s^2|^2} \tag{1}$$

$$T_{ab} = \frac{|t_{as}\phi_s\tau_{sb}|^2}{1 - |r_{sa}\rho_{sb}\phi_s^2|^2} \tag{2}$$

where r_{as} and t_{as} denote complex-amplitude reflection and transmission coefficients, respectively, when the light beam passes through the subsystem: medium *a*/implanted layer *l*/pristine film layer *f*/substrate *s*. When we successively apply the transfer matrix to this subsystem, the following expressions are obtained:

$$r_{as} = \frac{\rho_{al} + \phi_l^2\rho_{lf} + \rho_{fs}(\rho_{al}\rho_{lf}\phi_f^2 + \phi_l^2\phi_f^2)}{1 + \rho_{al}\phi_l^2\rho_{lf} + \rho_{lf}\phi_f^2\rho_{fs} + \rho_{al}\phi_l^2\phi_f^2\rho_{fs}} \tag{3}$$

$$t_{as} = \frac{\tau_{al}\phi_l\tau_{lf}\phi_f\tau_{fs}}{1 + \rho_{al}\phi_l^2\rho_{lf} + \rho_{lf}\phi_f^2\rho_{fs} + \rho_{al}\phi_l^2\phi_f^2\rho_{fs}} \tag{4}$$

where ρ and τ are Fresnel's complex-amplitude reflection and transmission coefficients, respectively. In $\phi_l = \exp(i\omega N_l d_l/c)$, N_l is the complex refractive index ($N_l = n_l + ik_l$) of the implanted layer, d_l is its thickness, and c is light velocity in vacuum. In eqs. (1) and (2), r_{sa} and t_{sa} are the corresponding coefficients, respectively, for the light through the same subsystem but with oppo-

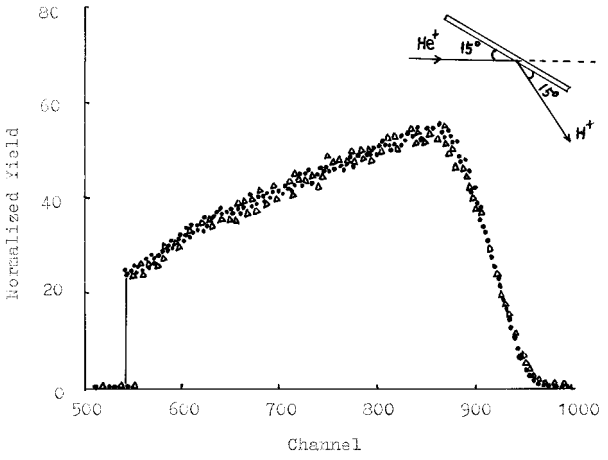

Figure 1 Recoil protons spectra from the plasma-polymerized pyrrole film (●) before and (△) after I^+-beam implantation. The energy and fluence of the I^+ beam were 20 keV and 1×10^{16} ions cm^{-2}, respectively.

site direction. Their expressions can also be given by the same approach. After substituting the experimental reflectance and transmittance data of the studied system into the above equations and calculating them by an iterative program, we can obtain the refractive index n_l and extinction coefficient k_l of the I^+-beam-implanted layer. (The complex refractive indices N_f of pristine film and N_s for substrate have been previously obtained from the corresponding reflectance and transmittance spectra by the transfer matrix method.) Because the complex dielectric function $\epsilon = \epsilon_1 + i\epsilon_2$ is related to complex refractive index by $\epsilon = N^2$, we then yielded the complex dielectric function of the I^+-beam-implanted layer according to $\epsilon_1 = n_l^2 - k_l^2$ and $\epsilon_2 = 2n_l k_l$.

RESULTS AND DISCUSSION

Ion Beam Analysis Techniques

The proton recoil spectra from the plasma-polymerized pyrrole film before and after I^+-beam implantation are reported in Figure 1. It shows that the ERD spectrum of the implanted sample coincides with the pristine film within the measurement error. Figure 2 represents the RBS spectrum of the I^+-beam-implanted sample. The positions of the surface channels for elements C, N, O, and I are marked by arrows in this figure. We have previously compiled a program to calculate a set of equations which relate the ratio of surface channel heights, either between the implanted sample and standard (Mylar films) for ERD spectra or between C, N, O, or I for RBS spectrum, to the elemental compositions.[7] Inputting the values of the surface channel yields for the spectra of the sample before and after I^+ implantation, respectively, into the program, we may obtain the atomic fractions after several iterations, as follows: $x_C = 0.50$, $x_H = 0.38$, $x_N = 0.11$, and $x_O = 0.01$ for the pristine film, and $x_C = 0.495$, $x_H = 0.376$, $x_N = 0.109$, $x_O = 0.01$, and $x_I = 0.01$ for the I^+-implanted layer. To compare the two sets of composition, we conclude that 20-keV I^+-beam implantation does not induce the variation of the contents of elements C, H, N, and O in the plasma polymer within the experimental precision. The formulae of the film before and after I^+ implantation can be written as $C_4H_{3.04}N_{0.88}O_{0.08}$ and $C_4H_{3.04}N_{0.88}O_{0.08}I_{0.08}$, respectively.

Using the equation $\Delta E = N[\varepsilon_0]_I \Delta x$ under the surface energy approximation, we estimated the thickness of I^+-beam-implanted layer to be about 69.4 nm, which is much larger than that evaluated from the TRIM-91 program. (According to TRIM-91, the average projective range and its struggle for 20-keV I^+ irradiation in the pristine film are 16.6 and 3 nm, respectively.) This means that the doping iodine atoms diffused during the carried-out charge transfer with the polymer. However, the charge transfer complex is considerably steady and the peak induced by iodine backscattering in the RBS spectrum has no detectable variation for the I^+-implanted sample after exposure to laboratory air for 6 mo. From

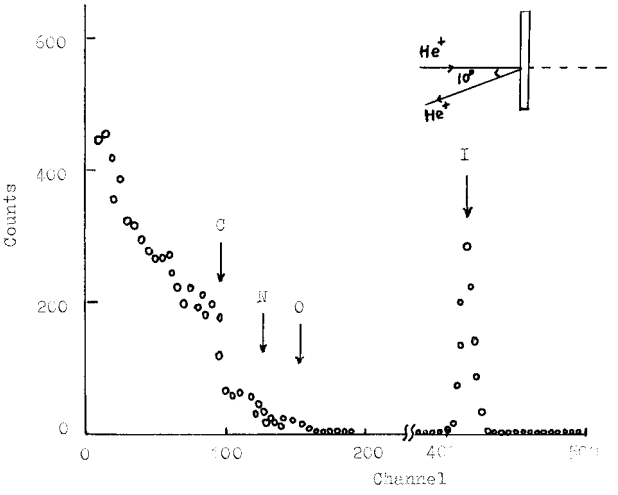

Figure 2 RBS spectrum of the I^+-beam-implanted plasma polymer film. The positions of the surface channels for the related elements are marked by arrows.

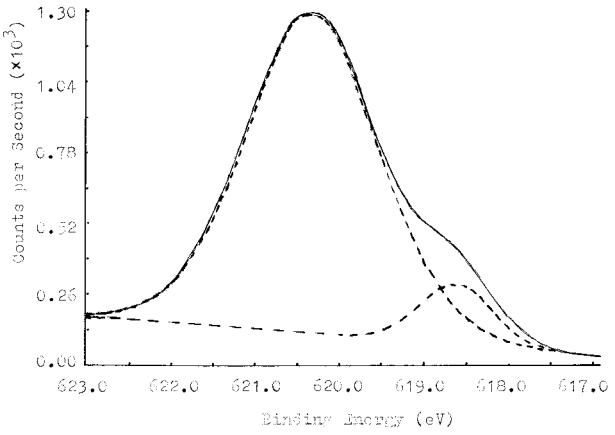

Figure 3 XPS I $3d_{5/2}$ core-level spectrum of the I^+-beam-implanted sample.

the iodine content (1.63×10^{21} cm^{-3}) and implanted layer thickness, the fluence of the I^+ beam is estimated equal to 1.1×10^{16} I^+ ions cm^{-2}. This coincidence with experimental fixation is satisfactory.

X-ray Photoelectron Spectroscopy

The ESCA analysis of plasma-polymerized pyrrole film has been previously reported elsewhere.[3] Similar to the pristine film, the C_{1s} core-level spectrum of the I^+-beam-implanted sample can be decomposed into three peaks: the main component peak located at 284.74 eV corresponds to α-C within pyrrole ring and unfunctionalized hydrocarbon CH_x; the peak at 283.89 eV can be assigned to β-C within pyrrole ring; and the peak at 285.99 eV corresponds to carbon atoms bonded with oxygen. The N_{1s} envelope is also divided into three fractional peaks, which are ascribed as follows: the main peak at 400.10 eV to the —NH— and C≡N; the peak at 398.6 eV to the =N— species; and the peak at 401.68 eV to the more positively charged nitrogen than —NH—. In the present paper, we will pay more attention to examining the nature of iodine species. In the case of iodine-doped materials it is possible to form different iodine species, such as I_2, I^-, I_3^-, I_5^-, or I_7^-.[8–11] The I $3d_{5/2}$ core-level spectrum for our sample after Ar^+ etching is shown in Figure 3. It is observed that two components can be decomposed in this spectrum. According to the studies of other authors concerning I_2-doped polyacetylene and polyphenylacetylene,[8,11] the main component at 620.33 eV with a proportion of 90.7% and the other at 618.60 eV could be ascertained to I_5^- and I_3^-, respectively. These anion species seem to be produced due to charge transfer between iodine and C=C double bonds within the pyrrole ring. However, nitrogen with unbonded pair electrons can stimulate this reaction. Similar to the conclusion of RBS, no apparent variation in the iodine core-level spectrum has been observed after exposing the implanted sample to laboratory air for 6 months.

Optical Constants of the Implanted Layer

It is known that the frequency-dependent complex dielectric constant is useful to describe the optical properties of a material. Its imaginary part is particularly important for exploring electronic structure because it can be related to electron transitions. Figure 4 shows the spectral dependences of ϵ_1 and ϵ_2 for the I^+-beam-implanted layer, which were obtained by the method mentioned earlier. Moreover, according to $\alpha_l = 4\pi k_l/\lambda$, the absorption coefficient α_l of the I^+-implanted layer was calculated as reported in Figure 5. For comparison, the absorption coefficient α_f of the sample before I^+ implantation is also represented in this figure. The spectral structures of α_f below 2 eV may be associated with localized electronic states within the gap. (The optical gap of pristine

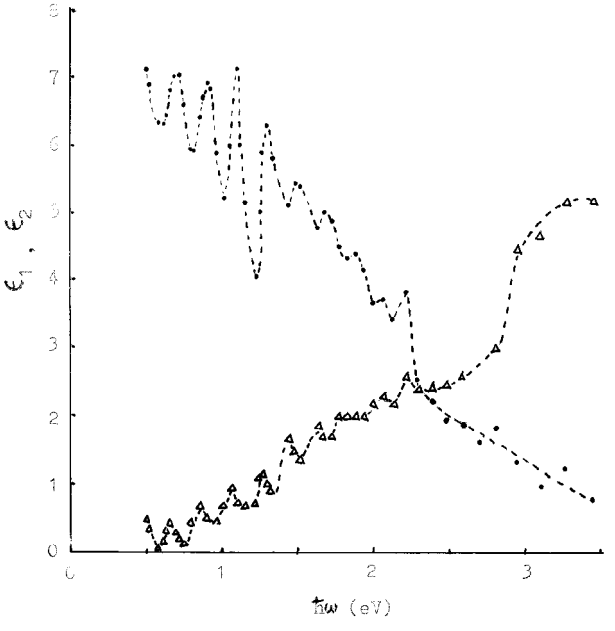

Figure 4 Spectral dependences of the (●) real part ϵ_1 and (△) imaginary part ϵ_2 of complex dielectric function for the I^+-beam-implanted layer. The thicknesses of implanted layer, pristine film layer, and substrate were 69.4 nm, 261 nm, and 10^3 μm, respectively.

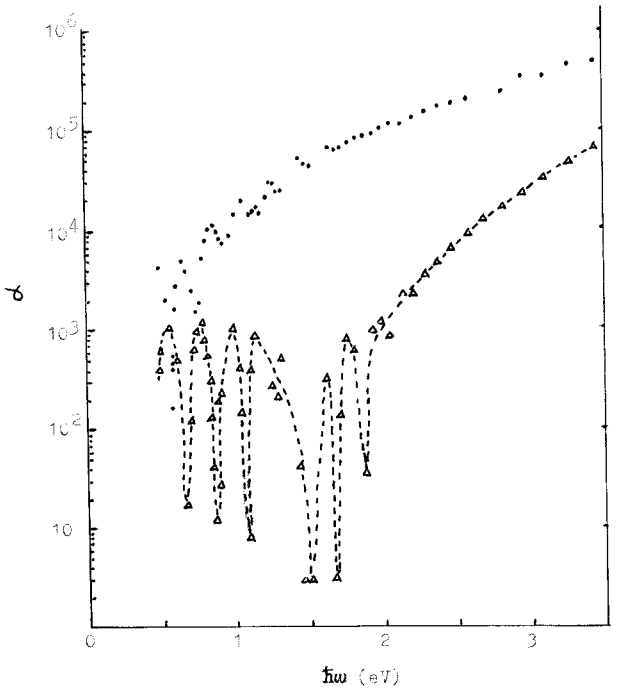

Figure 5 Plots of the absorption coefficient for (●) the I^+-beam-implanted layer and (△) the film before implantation.

film has been determined to equal 2.4 eV.[3]) These levels are in part attributable to charge transfer-induced modifications of the π system of the polymer. As shown above, our pristine film consists of a certain amount of oxygen which is known to be an acceptor dopant for polypyrrole.[12,13] Moreover, defects and disordering present in the plasma polymer can also introduce states into the gap.[13–15] Hence, the detailed interpretation of these spectral features may be conceivably complicated. However, it is seen that the six peaks occurred in the range of photon energies below 2 eV can be grouped into two sets: 0.55, 1.1, and 1.65 eV for the one; 0.78, 1, and 1.77 eV for the other. For each set the sum of the first two peak energies corresponds to the peak energy for the third transition. This result is consistent with the polaron theory model.

As shown in Figure 5, the optical absorption spectrum of the sample is obviously affected by the I^+-beam implantation. It is known that the basic feature of the electronic absorption spectrum for an acceptor-doped polymer is the formation of new broad band extending beyond the absorption edge of the polymer into the near-IR, and the whole spectrum from near-IR to UV is usually enhanced with the increasing doping levels.[12,16,17] According to Bredas and colleagues,[18] singly positively charged polarons are formed on the chains at low doping levels, and for each polaron two localized electronic levels are introduced in the gap: a singly occupied bonding polaron and an empty antibonding polaron state. At higher doping levels, two polarons combine to form a doubly charged spinless bipolaron which also introduces two states in the gap, but in contrast to the polaron case the bipolaron bonding state is empty. In addition, one should be aware that the levels associated with dopant counteranions are also conceivably incorporated into the energy band structure, resulting in additional electronic absorption. From the works on I_2-monosubstituted polyacetylene systems by other authors,[9,10] we know that the absorption peak locations associated with I_5^- and I_3^- species are around 2.76 and 3.4 eV, respectively. In the following, we shall apply the sum rule involving the imaginary part of complex dielectric function to further extract quantitative information concerning the electronic transitions.

Application of the Sum Rule

By calculating the sum rule[19]

$$n_{eff} = (2\epsilon_0 m/\pi e^2 \hbar^2 N) \int_0^{E_M} E\epsilon_2(E) dE \qquad (5)$$

we may obtain information on the effective number of electrons per molecule $C_4H_{3.04}N_{0.88}O_{0.08}$-$I_{0.08}$ contributing to the optical properties in the photon energy range up to E_M. Here ϵ_0 and m denote the dielectric constant in vacuum and electron mass, respectively; N is the molecule density in the I^+-beam-implanted layer. In eq. (5), except for $\hbar$, which is in eV s, and E, which is in eV, all quantities are in SI units. Because 20-keV I^+-beam implantation does not change the original elemental contents in the plasma polymer, the value of molecule density can be estimated from $N = (\rho_0 + \rho_I)N_A/M$, where ρ_0 is the density of pristine film; N_A is Avogadro's number; and ρ_I and M denote, respectively, the quantity of iodine per cubic meter and molar weight in the I^+-beam-implanted layer, which were obtained from the ion-beam analysis techniques as reported above. The values of n_{eff} for the implanted layer obtained using ϵ_2 of Figure 4 are shown in Figure 6. In this figure, n_{eff} of the film before I^+ implantation is also reported for examining the effect of dopant

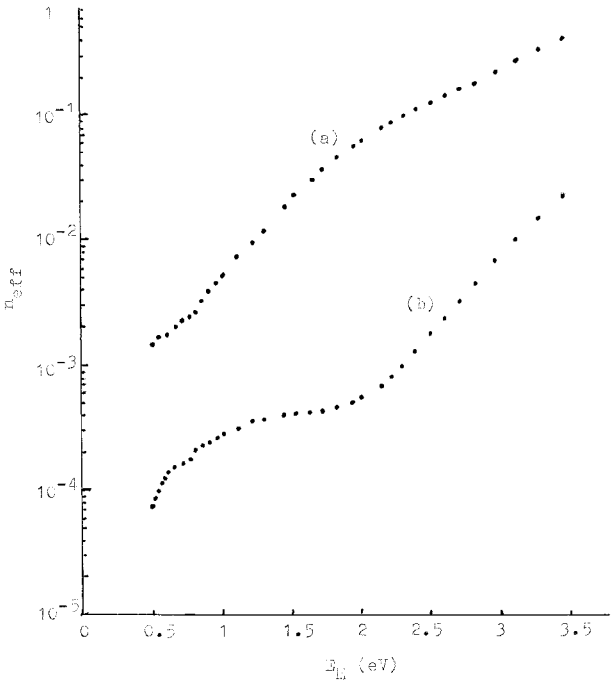

Figure 6 Plots of the effective number of electrons per molecule taking part in optical transitions in the range of photon energies up to E_M; curves (a) for the I^+-beam-implanted layer and (b) for the film before implantation.

iodine. It is of interest to note that the curve for pristine film appears to plateau at about $n_{eff} = 4 \times 10^{-4}$ around the photon energy 1.5 eV. It means the oscillator strength for transitions involving the states within the gap is exhausted before the interband π–π^* excitations are energetically possible. [Note: It considers that in the oxygen-doped polymers, the dopant oxygen is usually in the form of O_2^{2-} species.[13] From the value of n_{eff} at the plateau of Fig. 6, for every molecule $C_4H_{3.04}N_{0.88}O_{0.08}$ the ratio between the transition electron number observed within the gap and the number of oxygen molecule is to equal 10^{-2} ($= 4 \times 10^{-4}/0.04$). It means even if the transitions observed within the gap for the pristine film are induced exclusively by oxygen doping, there is only one counteranion O_2^{2-} per hundred of oxygen molecule. Therefore, only a very minor part of the incorporated oxygen acts as the dopant; a preponderant portion of incorporated oxygen is to form the oxygen-containing groups. This conclusion has been proved by Fourier transform infrared spectroscopy and XPS analyses in our previous article.[3]]

By contrast, the values of n_{eff} for the I^+-implanted layer are obviously larger than that of pristine film and sustain a steady rise with the increasing energies, instead of plateauing. Because of the low doping level, we suppose that the interband π–π^* transitions are apparently not affected by doping. The effective electron number per molecule $C_4H_{3.04}N_{0.88}O_{0.08}I_{0.08}$ concerning transitions involving the levels of either polaron or else dopant counteranion over the energy range up to 3.5 eV is then estimated from Figure 6 to equal 0.38 (=0.4–0.02). From the content of iodine, we know that there is one iodine atom per 12.5 molecules. Considering the proportion of I_5^- to the I_3^- species, we evaluated that on the average, every 60 molecules consists of a dopant counteranion; it implies each charge-transfer roughly induces 22.8 ($= 0.38 \times 60$) electrons to transit within the energy range up to 3.5 eV associated with the levels of either polaron or else dopant counteranion. This value seems too large and this evaluation should not be expected to be exact, since the spectral data have not been Kramers–Kronig transformed due to the limited spectral range. However, it at least shows some features on the optical properties as well as the corresponding electronic structures in the I^+-beam-implanted layer for the plasma polymer of pyrrole. It is known that the presence of two levels induced by a polaron may result in the following direct transitions of electrons (with either spin): transition from valence band to the two polaron levels, via polaron levels to conduction band, and transition from bonding polaron level to antibonding polaron level. Since the electron–phonon coupling is strong in the organic system and the transitions are usually accompanied by phonon processes, then the electron number of transitions should be more than that for direct transitions.

In the discussion above, the polaron model has been quoted to interpret the electronic transitions observed within the gap. But the plasma-polymerized materials are generally different from conventional polymers, more defects and severe disordering are present in the plasma polymers, and many monomer rings are subjected to destruction during the plasma process. It is well known that disorder can affect the electronic structure, resulting in the localization of states. If the disorder potential is large compared with the bandwidth, all states become localized. Otherwise the localized and extended states are separated by the mobility edge.[15,20] Considering the effects of defect and disordering, it is possible that for the acceptor-doped plasma polymers the localized electronic levels attributable to the modifications

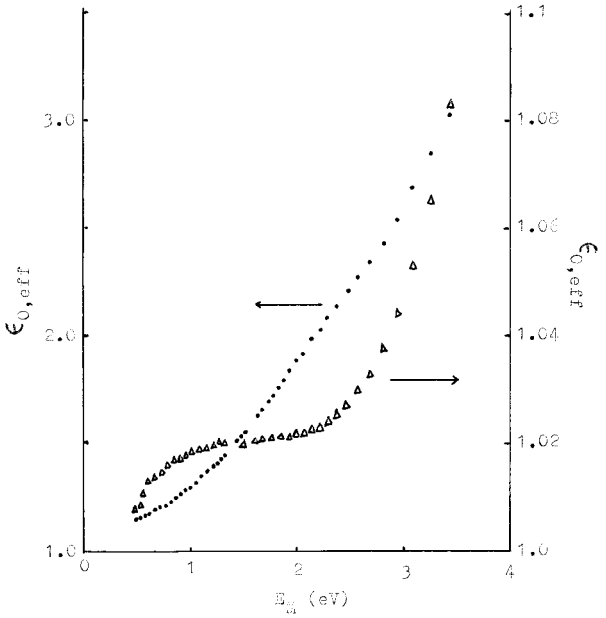

Figure 7 Plots of $\epsilon_{0,eff}$ for (●) the I^+-beam-implanted layer and (△) the film before implantation.

of the polymer's π system induced by local geometry modification resulting from charge-transfer should have some differences with respect to the polaron levels in the acceptor-doped polymers synthesized chemically or electrochemically. However, the essentials are the same for the two cases.

Another sum rule[19]

$$\epsilon_{0,eff} = 1 + \frac{2}{\pi}\int_0^{E_M} E^{-1}\epsilon_2(E)dE \qquad (6)$$

is for $\epsilon_{0,eff}$, the static or effective real dielectric constant produced by optical transitions in the energy range to E_M, which is obtained immediately from the Kramers–Kronig relations between the real and imaginary parts of complex dielectric function. The plots of $\epsilon_{0,eff}$ as a function of E_M for the plasma polymer of pyrrole before and after I^+ implantation are shown in Figure 7. From this figure, we see that the spectral features of the plots of n_{eff} are also obvious on these curves.

DC Electrical Conduction

The dc electrical conductivity at temperature 297 K for the pristine sample is of the order of 10^{-14} S cm^{-1}. After implantation of 20 keV I^+ at a fluence of 1×10^{16} ions cm^{-2}, the dc conductivity in the implanted surface layer increases to 1.7×10^{-3} S cm^{-1}. The analysis of the data shows that it is difficult to describe the temperature dependence of conductivity in terms of a single model over the whole experimental temperature range from 120 to 297 K. A reasonable analysis leads us to conclude that in the lower temperature region ($T \leq 200$ K), the conductivity can be well described in terms of the three-dimensional variable range hopping (3D-VRH)[20,21]

$$\sigma = K_0 T^{-1/2} \exp[-(T_0/T)^{1/4}] \qquad (7)$$

where $T_0 = 16\alpha^3/k_B N(E_F)$ and $K_0 = 0.39[N(E_F)/\alpha k_B]^{1/2}\nu_0 e^2$; α^{-1} is the decay length of the localized state, ν_0 is a hopping attempt frequency, and $N(E_F)$ is the density of states at the Fermi level. From Figure 8, we obtained $T_0 = 3.5 \times 10^7$ K and $K_0 = 5.6 \times 10^5$ S cm^{-1} $K^{1/2}$. Considering the severe disordering in the I^+-beam-implanted layer resulting not only from plasma etching during polymerization but also from iodine-ion bombardment, we believe the states in the gap are more localized. If we let $\alpha^{-1} = 0.1$ nm, we then obtain the yield $N(E_F) = 5.4 \times 10^{21}$ $eV^{-1}cm^{-3}$ and $\nu_0 = 1 \times 10^{16}$ s^{-1}. The value of ν_0 obtained in this article is larger than optical phonon frequency ν_{ph}. This result has also been obtained by other authors.[21,22] In order to correct the conductivity of

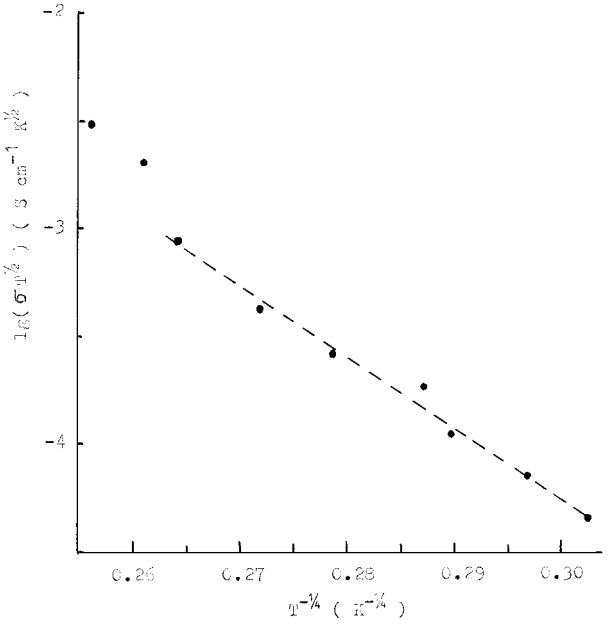

Figure 8 Mott plot of the dc conductivity for the I^+-beam-implanted layer in the temperature region from 119 to 200 K.

polyacetylene, Epstein and associates[22] assumed $\nu_0/\nu_{ph} = 130 \sim 690$. If we take their suggestion, our data gives a realistic value of ν_{ph} with the order of 10^{13} s^{-1}.

Using $p = N(E_F)k_BT$, we estimate the carrier concentration p to be about 0.9×10^{20} cm^{-3}. As an approximation, supposing all iodine ions in the I^+-beam-implanted layer are of the form I_5^- species, the concentration of I_5^- (i.e., the concentration of cation radicals on polymer backbone) is roughly evaluated to equal 3×10^{20} cm^{-3} from the result of ion-beam analysis, which approaches but is slightly larger than the magnitude of carrier concentration by conductive analysis. Substituting the values of σ and p into $\sigma = pe\mu$, the mobility of carriers may be estimated to be on the order of 10^{-6} cm^2 V^{-1} s^{-1}. This result coincides with the idea that for some conductive polymers, the low conductivity (e.g., within the order of 10^{-4} S cm^{-1}) is usually attributable to the low mobility (sometimes less than 10^{-7} cm^2 V^{-1} s^{-1}).[23,24]

According to the 3D-VRH model, the greatest possible hopping distance of the charge carriers can be calculated equal to 0.8 nm at temperature 160 K by the following equation:

$$R = \left[\frac{3}{2\alpha(4\pi/3)N(E_F)K_BT}\right]^{1/4}$$

This value of R is nearly two orders of magnitude lower than the thickness of the I^+-beam-implanted layer. That is the reason why the conductivity data can be described in terms of the VRH model in three dimensions.

In the higher temperature region (≥206 K), dc conductivity in the I^+-implanted layer is characterized by the multiphonon-assisted carrier hopping between localized states.[25] This model gives

$$\sigma = AT^{-3/2}\exp(-E_a/k_BT) \tag{8}$$

where

$$A = (e^2/6)(2\pi/\hbar)pR^2|V|^2(16\pi E_a)^{-1/2}k_B{}^{-3/2}$$

and p is the carrier concentration; V represents charge exchange integral $V = V_0\exp(-\alpha R)$, with V_0 usually in the range of 5 to 20 eV. From Figure 9, we immediately obtained $E_a = 0.24$ eV and $A = 1.1 \times 10^5$ S $cm^{-1}K^{3/2}$. Substituting $p = 1 \times 10^{20}$ cm^{-3} and $V_0 = 50$ eV into the formula of A, α^{-1} was yielded approximately equal to 0.2 nm. From the report of Nishio and coworkers,[26] the dc conductivity of plasma-polymerized 1-benzothiophene thin film can be analyzed by the 3D-VRH model in the lower temperature region (<170 K) and is fitted using the Arrhenius equation with an activation energy of 0.27 eV in the higher temperature region (>250 K). Our work on the temperature dependence of conductivity reported in this article coincides with the results obtained by Nishio and associates.[26]

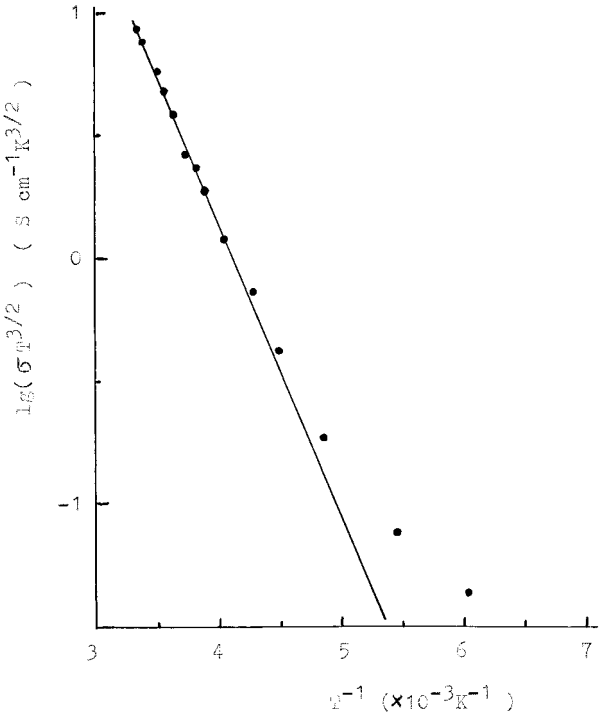

Figure 9 Logarithmic plot of $\sigma T^{3/2}$ versus T^{-1} for the I^+-beam-implanted layer in the temperature region from 206 to 297 K.

CONCLUSIONS

The composition of the plasma-polymerized pyrrole film implanted with an iodine ion beam of 20 keV energy at a fluence of 1×10^{16} ions cm^{-2} was determined by ion-beam analysis techniques, whose formula obtained from this determination can be represented as $C_4H_{3.04}N_{0.88}O_{0.08}I_{0.08}$. The thickness of the I^+-beam-implanted layer was estimated equal to 69.4 nm, which is larger than that calculated from TRIM-91 due to the diffusion of iodine. The implanted iodine ions carried out charge transfer with polymer backbone to produce I_5^- species with a proportion of 90.7% and I_3^- species with the residual fraction. The electron

absorption spectrum shows that the number of electrons participating in transitions can be enhanced by at least one order of magnitude due to I^+-beam implantation and sustains a steady rise with the increasing energies over the whole experimental energy region. These excess electrons with respect to the original plasma polymer film are associated with transitions involving the levels of either polaron or else dopant counteranion, all of which result from the charge transfer.

The dc electrical conductivity at room temperature is of the order of 10^{-14} S cm^{-1}. Implantation of a 20-keV iodine-ion beam at the fluence of 1×10^{16} ions cm^{-2} enhance the conductivity to 1.7×10^{-3} S cm^{-1}. The temperature dependence of conductivity can be described by the 3D-VRH model for the lower temperature region, whereas the transport process of charge carriers in the higher temperature region may be analyzed in terms of multiphonon-assisted carrier hopping between localized states.

The authors are indebted to professors Miao Chen and Zhi Yi Zhou for their excellent technical assistance in the ion implantation. Near-IR to UV spectra were recorded at the Shanghai Institute of Optics and Fine Mechanics, Chinese Academy of Sciences. XPS was performed at the Shanghai Institute of Iron and Steel Research. This work is supported by the National Natural Science Foundation of China under Award No. 19375036, for which the authors also express their gratitude.

REFERENCES

1. J. R. Ferraro and J. M. William, *Introduction to Synthetic Electrical Conductors,* Academic Press, New York, 1987.
2. G. Q. Yu and M. Thakur, *J. Polym. Sci., Part B, Polym. Phys. Ed.,* **32,** 2099 (1994).
3. J. Zhang, M. Z. Wu, T. S. Pu, Z. Y. Zhang, R. P. Jin, Z. S. Tong, D. Z. Zhu, D. X. Cao, F. Y. Zhu, and J. Q. Cao, *Thin Solid Films,* **307,** 14 (1997).
4. K. Tanaka, K. Yoshizawa, T. Takeuchi, T. Yamabe, and J. Yamauchi, *Synth. Met.,* **38,** 107 (1990).
5. N. Savvides, *J. Appl. Phys.,* **59,** 4133 (1986).
6. B. Harbecke, *Appl. Phys. B,* **39,** 165 (1986).
7. Z. S. Tong, M. Z. Wu, T. S. Pu, J. Zhang, Z. Y. Zhang, R. P. Jin, D. Z. Zhu, F. Y. Zhu, D. X. Cao, and J. Q. Cao, *Appl. Surf. Sci.,* **119,** 93 (1997).
8. G. Polzonetti, A. Furlani, M. V. Russo, A. M. Camus, and N. Marsich, *J. Electron Spectrosc. Related Phenom.,* **52,** 581 (1990).
9. M. A. Petit and A. H. Soum, *J. Polym. Sci., Part B, Polym. Phys. Ed.,* **25,** 423 (1987).
10. C. Cametti, A. Furlani, G. Iucci, and M. V. Russo, *Synth. Met.,* **68,** 259 (1995).
11. S. L. Hsu, A. J. Signorelli, G. P. Pez, and R. H. Baughman, *J. Chem. Phys.,* **69,** 106 (1978).
12. P. Pfluger, M. Krounbi, G. B. Street, and G. Weiser, *J. Chem. Phys.,* **78,** 3212 (1983).
13. J. C. Scott, P. Pfluger, M. T. Krounbi, and G. B. Street, *Phys. Rev. B,* **28,** 2140 (1983).
14. Z. Ovadyahu, *Phys. Rev. B,* **47,** 6161 (1993).
15. K. Lee, A. J. Heeger, and Y. Cao, *Synth. Met.,* **72,** 25 (1995).
16. Y. Cao, *Synth. Met.,* **35,** 319 (1990).
17. M. Thakur and B. S. Elman, *J. Chem. Phys.,* **90,** 2042 (1989).
18. J. L. Bredas, J. C. Scott, K. Yakushi, and G. B. Street, *Phys. Rev. B,* **30,** 1023 (1984).
19. H. R. Philipp and H. Ehrenreich, *Phys. Rev.,* **129,** 1550 (1963).
20. N. F. Mott and E. A. Davis, *Electronic Processes in Non-Crystalline Materials,* Clarendon Press, Oxford, 1979, p. 32.
21. K. Sato, M. Yamaura, T. Hagiwara, K. Murata, and M. Tokumoto, *Synth. Met.,* **40,** 35 (1991).
22. A. J. Epstein, H. Rommelmann, R. Bigelow, H. W. Gibson, D. M. Hoffmann, and D. B. Tanner, *Phys. Rev. Lett.,* **50,** 1866 (1983).
23. R. H. Baughman, J. L. Bredas, R. R. Chance, R. L. Elsenbaumer, and L. W. Shackette, *Chem. Rev.,* **82,** 209 (1982).
24. M. Stolka, J. F. Yanus, and D. M. Pai, *J. Phys. Chem.,* **88,** 4707 (1984).
25. E. Buhks and I. M. Hodge, *J. Chem. Phys.,* **83,** 5976 (1985).
26. S. Nishio, T. Takeuchi, Y. Matsuura, K. Yoshizawa, K. Tanaka, and T. Yamabe, *Synth. Met.,* **46,** 243 (1992).